Anomalous absorption of proton partial waves by the optical potential

Y. Iseri and M. Kawai
Department of Physics, Kyushu University, Fukuoka 812, Japan
(Received 10 February 1986)

Anomalous absorption of proton partial waves by the nuclear optical potential is investigated for all the stable target nuclei over the range of energy 0–80 MeV and orbital angular momentum 0–13. It occurs with striking regularity very similar to those found for the neutron except that the $l=0$ anomalies are associated with resonance poles rather than antibound state poles, and the target-nucleus dependence of the anomaly is quite different. The latter is shown to be due to the symmetry term of the optical potential.

I. INTRODUCTION

In a previous paper,[1] hereafter referred to as I, we reported on anomalously strong absorption of neutron partial waves by the nuclear optical potential which occurs for certain combinations of the target nucleus, the incident energy, and the angular momentum of the partial wave. We called the phenomenon "anomalous absorption" and investigated it in detail. We mentioned that anomalous absorption is likely to occur not only for neutrons, but also for other, charged, light projectiles.

In the present paper we report on anomalous absorption for a proton. The definition of anomalous absorption is qualitatively the same for a charged particle as for a neutron: approximate absence of the outgoing wave in a partial wave. Quantitatively, however, it is slightly complicated because of the Coulomb potential. We give it in the following way. Let $u_{lj}(k,r)$ be a radial wave function of a partial wave with wave number k and orbital and total angular momenta l and j, respectively. The asymptotic form of $u_{lj}(k,r)$ is given by

$$u_{lj}(k,r)\sim u_l^{(-)}(k,r)-S_{lj}^N(k)u_l^{(+)}(k,r)\ , \tag{1}$$

where $S_{lj}^N(k)$ is the so-called nuclear part of the S-matrix element and $u_l^{(\pm)}(k,r)$ are the outgoing and incoming Coulomb wave functions with the asymptotic forms

$$u_l^{(\pm)}(k,r)\sim\exp\{\pm i[kr-\eta\ln 2kr+\sigma_l(\eta)+l\pi/2]\}\ , \tag{2}$$

where η is the Sommerfeld parameter and $\sigma_l(\eta)$ is the Coulomb phase shift. Now, the outgoing wave part of $u_{lj}(k,r)$ becomes very small whenever $S_{lj}^N(k)$ gets close to zero. Thus, one can define anomalous absorption by the smallness of $|S_{lj}^N(k)|$.

The nuclear part of the S-matrix element is related to the total S-matrix element $S_{lj}(k)$ including the Coulomb phase shift through

$$S_{lj}(k)=e^{2i\sigma_l(\eta)}S_{lj}^N(k)\ . \tag{3}$$

Hence, zeros of $S_{lj}^N(k)$ coincide with those of $S_{lj}(k)$ if $e^{2i\sigma_l(\eta)}$ is finite, which is actually the case in the domain of present interest in the complex k plane, in particular on the real k axis. Thus, one can define anomalous absorption in terms of the total S-matrix element as well.

We have made a search for anomalous absorption of proton partial waves for all the stable target nuclei and energies below 80 MeV, assuming the optical potential of Becchetti-Greenlees.[2] The result is summarized in Sec. II. As shown there, anomalous absorption occurs for various combinations of target nucleus, energy, and angular momentum, with regularities which are very similar to those found for a neutron. There are, however, some notable differences in the two cases. One of them is in the nature of $l=0$ anomalous absorption. As described in I, an $l=0$ anomaly for a neutron is associated with an anti-bound-state pole. For a proton, however, it is related to both a resonance pole and a bound state pole, and not to an anti-bound-state pole. Another difference is in the target nucleus dependence of the anomaly. Its dependence on the neutron and proton numbers of the target nucleus, N and Z, respectively, are almost opposite for a neutron and proton. The cause of this difference turns out to be the symmetry term of the optical potential. Detailed discussions on these and other salient features of the anomaly are given in Sec. III. A summary and conclusions of the work are given in Sec. IV.

II. SEARCH FOR ANOMALOUS ABSORPTION

The search for anomalous absorption is made for N and Z covering all the stable nuclei, and over the range of center-of-mass energy $0<E\lesssim 80$ MeV, orbital angular momentum $0\leqq l\leqq 13$, and total angular momentum $j=l\pm\frac{1}{2}$. For each set of (N,Z,E,l,j) the S-matrix element $S_{lj}^N(k)$ with $k=(2\mu E/\hbar^2)^{1/2}$ is calculated for the Becchetti-Greenlees proton optical potential with the parameters obtained from the formulae given in Ref. 2. The criterion of anomalous absorption is set to be $|S_{lj}^N(k)|<0.05$.

Figure 1 shows the distribution of the anomaly on the (N,Z) plane. One sees clusters of anomaly which fall into eight distinct groups, each of which lines up in the order of consecutive values of l. This is in complete analogy with the corresponding plot in I for neutrons. Table I lists the minimum value of $|S_{lj}^N(k)|$ in each cluster. Distribution of the anomaly on the (E,Z) and (l,E) planes, not illustrated here, also looks very similar to the corresponding distribution for a neutron shown in I.

Another striking regularity is seen in Fig. 2, which shows the distribution of the anomaly listed in Table I on the $(R_C, A^{1/3})$ plane with $R_C \equiv \{\eta + [\eta^2 + l(l+1)]^{1/2}\}/k$ discussed in Sec. III. Each of the six groups of anomalies seen in Fig. 1 now forms a very nearly straight line. This is analogous to the similar plot for neutron anomalous absorption on the $(l/k, A^{1/3})$ plane, Fig. 9 in I. The only difference is the modification of the ordinate to account for the Coulomb potential. We discuss this point further in the next section.

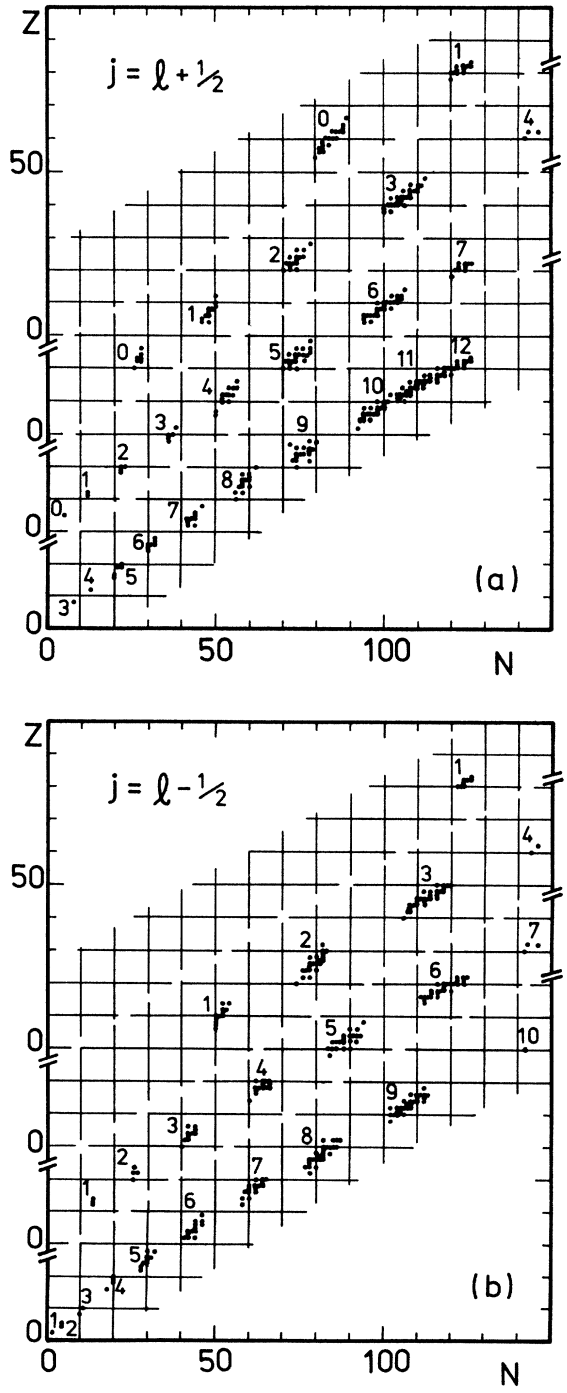

FIG. 1. Distribution of anomalous absorption on the (N,Z) plane of target nuclides. Anomalies with $j = l + \frac{1}{2}$ and $l - \frac{1}{2}$ are plotted separately in (a) and (b), respectively, each labeled by its l values. They are classified into series, each with consecutive l and plotted on different ordinates.

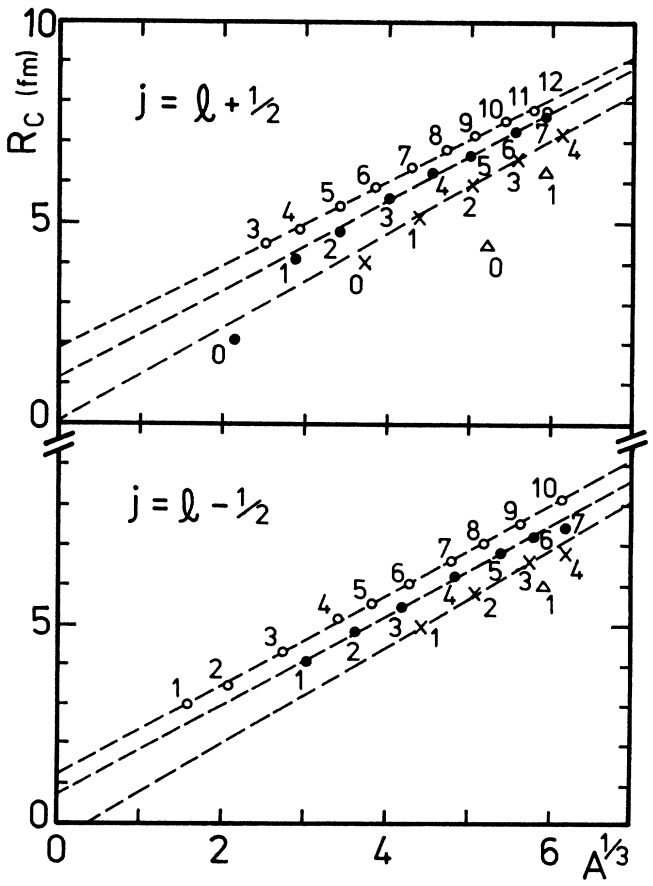

FIG. 2. Distribution of anomalous absorption on the $(R_C, A^{1/3})$ plane. The numbers indicate the l of the anomaly.

III. DISCUSSION

The features of anomalous absorption of proton partial waves described in Sec. II are basically very similar to those found in the neutron case. There are, however, some differences, too. In this section we discuss some characteristic features of the anomaly.

A. Classification of anomalous absorption

It was shown in I that for a neutron there are two types of anomalous absorption, type R and type A, according to the kind of pole with which the zero of the S-matrix element causing anomalous absorption is associated. A type R anomaly is associated with a resonance pole, and type A with an anti-bound-state pole.

One can classify anomalous absorption for a proton in the same way as for a neutron because the following equations, which are the basis of the classification, also hold for the proton:

$$S_{lj}(k,U)\cdot S^*_{lj}(k^*,U^*)=1 \qquad (4)$$

TABLE I. Summary of the minimum value of $|S_{lj}^{N}|$ in each cluster of points in Fig. 1. The $\pm$ correspond to $j = l \pm \frac{1}{2}$, η stands for the Sommerfeld parameter, and n the number of "nodes" of the wave function at the anomaly discussed in Sec. III. The numbers in the parentheses in the eighth column represent minus the power of 10 by which the preceding number is multiplied. The B and R in the last column stand, respectively, for the bound-state-pole and resonance-pole types of the anomaly discussed in Sec. III.

$l(\pm)$	A	Z	N	k (fm^{-1})	$E_{\text{c.m.}}$ (MeV)	η	$\lvert S \rvert$	n	Type
0(+)	10	5	5	0.389	3.454	0.406	2.531(2)	1	B
	52	24	28	0.637	8.581	1.283	5.630(3)	2	B
	142	58	84	0.858	15.382	2.329	1.008(3)	3	B
1(+)	24	12	12	0.561	6.802	0.713	1.517(2)	1	R
	85	37	48	0.756	11.998	1.679	1.516(3)	2	R
	209	83	126	0.985	20.227	2.910	4.011(4)	3	R
1(−)	4	2	2	0.509	6.719	0.109	3.608(2)	0	R
	28	14	14	0.589	7.455	0.796	7.534(3)	1	R
	87	37	50	0.769	12.411	1.651	1.810(4)	2	R
	208	82	126	1.000	20.848	2.832	1.886(2)	3	R
2(+)	40	18	22	0.718	10.964	0.849	1.100(2)	1	R
	128	54	74	0.892	16.638	2.084	2.329(3)	2	R
	9	4	5	0.754	13.106	0.166	7.801(3)	0	R
	48	22	26	0.747	11.819	1.001	6.326(3)	1	R
	132	54	78	0.906	17.160	2.053	8.354(4)	2	R
3(+)	16	8	8	0.845	15.741	0.309	3.285(2)	0	R
	65	29	36	0.860	15.582	1.152	6.676(4)	1	R
	176	71	105	1.013	21.412	2.418	6.778(4)	2	R
3(−)	21	10	11	0.886	17.063	0.374	1.842(2)	0	R
	74	32	42	0.893	16.769	1.227	1.058(3)	1	R
	191	77	114	1.040	22.559	2.556	1.370(3)	2	R
4(+)	25	12	13	1.012	22.099	0.396	2.483(2)	0	R
	96	42	54	0.989	20.506	1.458	3.665(3)	1	R
	232	90	142	1.122	26.232	2.771	3.471(3)	2	R
4(−)	40	20	20	1.001	21.310	0.676	1.192(2)	0	R
	113	49	64	1.025	21.992	1.644	3.306(4)	1	R
	238	92	146	1.170	28.522	2.717	3.360(2)	2	R
5(+)	40	19	21	1.127	27.012	0.571	1.193(2)	0	R
	126	52	74	1.101	25.351	1.626	2.913(3)	1	R
5(−)	56	26	30	1.136	27.254	0.780	3.920(3)	0	R
	156	66	90	1.143	27.280	1.991	2.505(3)	1	R
6(+)	57	26	31	1.236	32.253	0.717	4.577(3)	0	R
	170	70	100	1.211	30.607	1.994	1.383(3)	1	R
6(−)	79	35	44	1.239	32.254	0.968	2.875(3)	0	R
	196	78	118	1.243	32.221	2.166	7.978(4)	1	R
7(+)	80	36	44	1.329	37.105	0.928	3.860(3)	0	R
	208	82	126	1.309	35.723	2.163	1.402(2)	1	R
7(−)	110	48	62	1.329	36.980	1.242	4.299(3)	0	R
	238	92	146	1.357	38.367	2.343	2.624(2)	1	R
8(+)	105	46	59	1.423	42.414	1.111	1.483(3)	0	R
8(−)	140	58	82	1.417	41.958	1.410	8.805(4)	0	R
9(+)	130	54	76	1.513	47.862	1.229	2.307(3)	0	R
9(−)	180	73	107	1.498	46.818	1.682	1.181(4)	0	R
10(+)	160	64	96	1.596	53.181	1.383	3.489(3)	0	R
10(−)	232	90	142	1.556	50.451	1.998	4.101(2)	0	R

TABLE I. (*Continued*).

$l(\pm)$	A	Z	N	k (fm^{-1})	$E_{c.m.}$ (MeV)	η	$\|S\|$	n	Type
11(+)	193	77	116	1.692	59.707	1.571	2.249(4)	0	R
12(+)	209	83	126	1.831	69.893	1.565	1.278(2)	0	R
13(+)	238	92	146	1.920	76.808	1.659	3.224(3)	0	R

and

$$S_{lj}(k,U)\cdot S_{lj}(-k,U)=1\ , \tag{5}$$

where $S_{lj}(k,U)$ is the S-matrix element for a potential U, and the asterisks signify complex conjugate. If U is real, Eq. (4) reduces to

$$S_{lj}(k)\cdot S^{*}_{lj}(k^{*})=1\ . \tag{6}$$

Now, a simple way of determining the type of a zero of $S_{lj}(k)$ causing anomalous absorption is to see how it moves in the complex-k plane when the imaginary part of the optical potential is artificially turned off. One can do this if one multiplies the imaginary potential by an auxiliary constant N_I and changes it from 1 to 0. The anomaly is of type R if the zero moves to a point, say k_0, in the first quadrant since there is a pole at k_0^{*} in the fourth quadrant, a resonance pole according to Eq. (6). It is of type A if the zero moves to a point, say k_1, on the positive imaginary axis because the conjugate pole at $k_1^{*}=-k_1$ is an anti-bound-state pole on the negative imaginary axis. Figure 3 shows typical examples of the locus of the zero on the complex-k plane under such operation. Curve (a) is a locus for $l=0$. The zero moves on the curve from point A, nearly on the real axis, to point P in the first quadrant as N_I changes from 1 to 0.

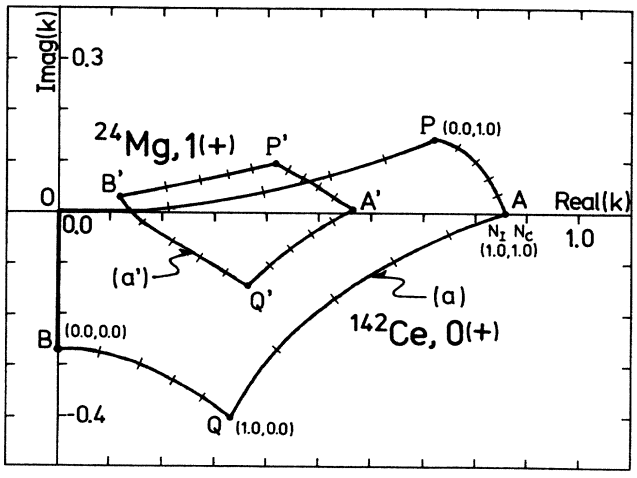

FIG. 3. The locus of zero corresponding to anomalous absorption on the complex-k plane when the values of N_I and N_C, indicated as (N_I,N_C), are changed. Curve $APBQ$ corresponds to $l=0$, $j=\frac{1}{2}$ on ^{142}Ce, and curve $A'P'B'Q'$ to $l=1$, $j=\frac{3}{2}$ on ^{25}Mg. An interval on the curves corresponds to a change of N_I or N_C by 0.2.

Hence, the anomaly is of type R. Curve (a') is a locus for $l\neq 0$. Again, the zero is at P', a point in the first quadrant, when $N_I=0$. Hence, the anomaly is of type R. Thus one sees that anomalous absorption is always of type R. This is in contrast to the case of a neutron in which all the zeros for $l=0$ are of type A.

It is evident that the difference stems from the Coulomb potential in the proton optical potential. It is therefore interesting to see what happens when the Coulomb potential, as well as the imaginary potential, is artificially turned off. This can be done by an auxiliary constant N_C which multiplies the Coulomb potential and changes from 1 to 0. If this is done after N_I is reduced to 0, the zero for $l=0$ moves on curve (a) in Fig. 3 from P to B, going through $k=0$ tangentially to the real-k axis. This movement of the zero is elucidated in the Appendix. Point B is on the negative imaginary axis. Hence, the pole associated with it is on the positive imaginary axis, i.e., a bound-state pole. One might therefore call this type of anomaly B, standing for bound state, the notation used in Table I instead of R.

B. Series of anomaly and "node" of wave function

In the preceding section we saw that the anomalies fall into eight distinct series. It turns out that each of the series corresponds to a definite number of oscillations in the modulus of the corresponding wave function inside the potential well. Examples of such oscillations are illustrated in Figs. 4(a), 4(b), and 4(c) for $n=0$, 1, and 2, respectively, where n is the number of minima in the oscillation except the one at the origin. All the anomalies on the top lines in Fig. 2 have wave functions with $n=0$, those on the next line below $n=1$, etc., down to those at the bottom with $n=3$.

The number n would obviously be a number of nodes of the wave function if the potential were real. Because of the Levinson theorem, therefore, the S-matrix element suffers a discrete jump every time n changes by an integer.[3] This explains why anomalies with different n lie on distinct lines. For quantitative understanding, however, further investigation is clearly needed. Exactly the same correspondence exists between n and the lines of anomaly for a neutron shown in Fig. 9 in I.

C. Coulomb modification of "distance of closest approach"

The ordinate of Fig. 2 accounts for the Coulomb interaction between the incident proton and the target nucleus through the parameter η. The ordinate is actually "the distance of closest approach," R_C, to the Coulomb

plus centrifugal potential at wave number k of the anomaly, satisfying

$$2\eta k/R_C+l(l+1)/R_C^2=k^2\ , \tag{7}$$

which gives

$$R_C=\{\eta+[\eta^2+l(l+1)]^{1/2}\}/k\ . \tag{8}$$

For a neutron $\eta=0$, and R_C reduces to $\sqrt{l(l+1)}/k\simeq l/k$ for large l, the ordinate of the corresponding plot for the neutron shown in I. Figure 2 shows the approximate linearity of R_C in $A^{1/3}$,

$$R_C=r_1A^{1/3}+\delta\ . \tag{9}$$

For the six lines in the figure, (r_1,δ) equals, from top to the bottom, (1.04,1.85), (1.12,1.05), (1.16,0.05) for $j=l+\frac{1}{2}$ and (1.13,1.22), (1.13,0.73), (1.22,−0.44) for $j=l-\frac{1}{2}$, respectively. If the Coulomb modification is not made, the lines in Fig. 2 become curvilinear.

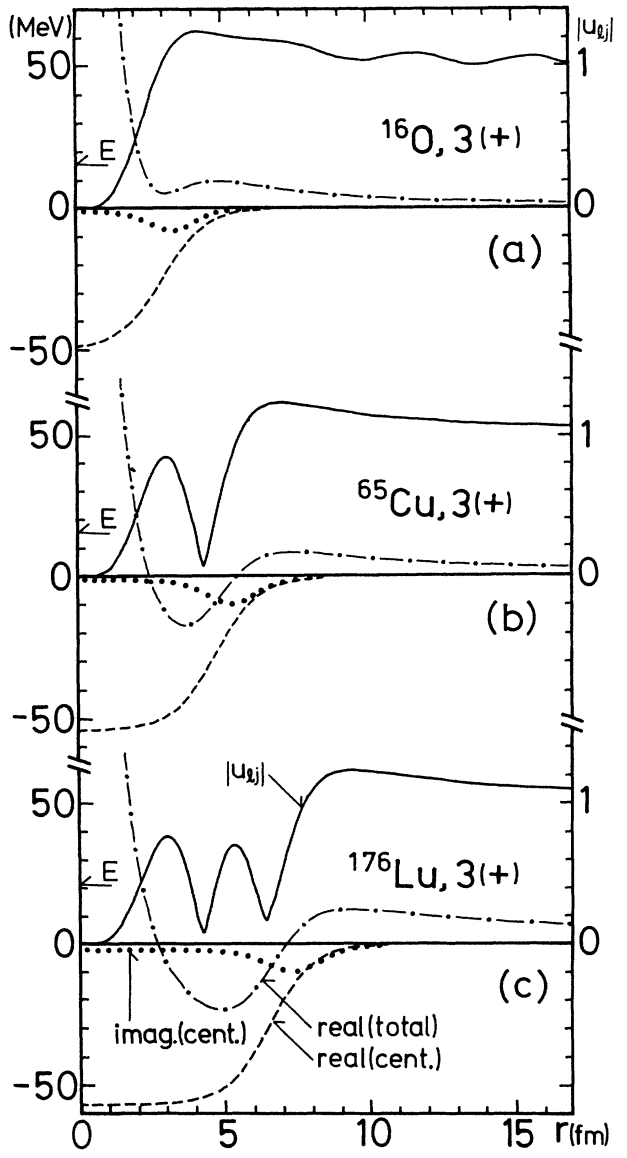

FIG. 4. The modulus $|u_{lj}(k,r)|$ for $l=3$, $j=\frac{7}{2}$ partial waves on ^{16}O, ^{65}Cu, and ^{176}Lu as a function of r, and the corresponding optical potentials. Solid lines represent $|u_{lj}(k,r)|$ with the right-hand-side ordinates in arbitrary units. Other lines represent different parts of the optical potential with the left-hand-side ordinates: the real central nuclear part (dashed lines), the real nuclear part plus the Coulomb and centrifugal potentials (dashed-dotted lines), and the imaginary part (dotted lines). The incident energy is indicated as E.

D. Target-nucleus dependence of anomalous absorption

It has been mentioned in I that the occurrence of anomalous absorption of neutron partial waves is more sensitive to Z than N of the target nucleus. For proton partial waves the opposite turns out to be true: the anomaly is more sensitive to N than Z. In fact, actual calculations show that the minimum value of $|S_{lj}^N|$ as a function of E depends roughly only on Z for a neutron and, to a lesser degree, only on N for a proton. One can also recognize this difference in the subtle difference between Fig. 1 of I and Fig. 1 of the present paper, which both show the distribution of anomalous absorption in the (N,Z) plane. The clusters of the anomalies look roughly parallel to the N axis in the former, while somewhat thick in the Z direction in the latter.

The cause of this difference is the symmetry potential in the Becchetti-Greenlees potential with the depth of the real central, and surface imaginary parts given by

$$V_{0,\mathrm{sym}}=\pm 24.0\frac{N-Z}{A}$$

and (10)

$$W_{s,\mathrm{sym}}=\pm 12.0\frac{N-Z}{A}\ ,$$

respectively, where the + and − signs refer to the proton and neutron, respectively. If it were not for this potential, the optical potential for the neutron would depend only on $A=N+Z$, and so would $|S_{lj}|$. Hence, the S matrix would depend equally on N and Z. The same would also be true for the proton, though only approximately because of the Coulomb potential, the $Z/A^{1/3}$ dependence part of the real nuclear potential, and the weak dependence of the diffuseness parameters on $(N-Z)/A$.

The symmetry potential violates the symmetric dependence of the S-matrix element on N and Z. To what extent it does depends on its strength. The actual strength is such that the S-matrix element depends roughly only on Z for the neutron and on N for the proton, as already mentioned. The opposite dependence on N and Z in the two cases is what is expected from the opposite sign and equal strength of the symmetry potential for the neutron and proton.

The explanation described above might seem somewhat surprising since the symmetry potential looks to be only a minor part of the optical potential. Actual calculations show, however, that the (N,Z) dependence of the S-matrix element is quite similar to that of the quantity $V_0R_0^2$, both for the neutron and proton, where V_0 is the

depth and R_0 is the radius of the real part of the central potential. This quantity is empirically known to be a parameter which "governs" the elastic scattering cross section.[4] For the neutron, $V_0R_0^2$ stays virtually constant when N is changed if Z is kept constant. This is because the change in the depth V_0 is compensated by the change in the radius R_0. The same is true for $V_0R_0^2$ for the proton if the roles of N and Z are interchanged. Thus we conclude that the change in the real central potential caused by the symmetry potential is large enough to explain why anomalous absorption for the neutron (proton) is sensitive only to Z (N).

IV. SUMMARY AND CONCLUSION

Anomalous absorption is seen in proton partial waves as well as in neutron partial waves in the scattering by the nuclear optical potential.

There are remarkable regularities in the occurrence of the anomaly. When plotted in the space of various combinations of the parameters (E,l,j,N,Z), the anomalies form eight distinct groups, each forming a smooth line. In particular, the lines on the $(R_C,A^{1/3})$ plane, where R_C is the distance of closest approach, are very nearly straight.

There is a correspondence between the lines of Fig. 2 and the number of "nodes," n, of the wave function at the anomaly, i.e., the number of oscillations of the modulus of the wave function inside the potential well. All the anomalies on the uppermost lines correspond to $n=0$, the next lines below to $n=1$, etc., down to the bottom lines corresponding to $n=3$. The same correspondence exists also in neutron anomalous absorption.

All these features of proton anomalous absorption are analogous to those of neutron anomalous absorption. They strongly suggest that same common features of the wave function are responsible for all the anomalies. There are, however, some noticeable differences, too, between the cases of the proton and neutron.

One difference is in the "type" of $l=0$ anomalies: type A for neutron and type R for proton. The zero of anomalous absorption for the proton turns into the complex conjugate of a resonance pole when the imaginary part of the optical potential is artificially turned off. When the Coulomb potential is also turned off the zero becomes the complex conjugate of a bound state pole. Hence the notation B used in Table I.

Another important difference is the target-nucleus dependence of the anomaly: it is sensitive to Z for the neutron and to N for the proton. The cause of this is the symmetry potential in Becchetti-Greenlees potential, which has the same magnitude and opposite signs for a neutron and proton. For the neutron (proton) a change in N (Z) causes little change in the S-matrix element, because the effect of the change in the potential depth is just cancelled by the effect of the change in the radius.

Finally, experimental observation of anomalous absorption might be easier for a proton, a charged particle, than for a neutron. For example, proton elastic scattering data may be analyzed in phase shifts which would reveal anomalous absorption, provided the phase shifts are uniquely determined. No drastic anomaly is expected to be recognized in the cross section or in the polarization quantities of the elastic scattering because, as already mentioned in I, anomalous absorption occurs only in one of the many partial waves contributing to those quantities. Also, it occurs rather gradually with respect to energy, with a half-width of order one MeV or so. Therefore, experiments which single out the particular partial wave seem to be necessary in order to directly observe the anomaly. In any case, if a systematic observation of the anomaly is done for a neutron and proton, it will give interesting information on the optical potential, particularly on its symmetry potential.

ACKNOWLEDGMENTS

The authors wish to thank Professor N. Austern, and a number of experimental people, especially Professor T. Nomura and Dr. T. Motobayashi, for their interest in this work and valuable discussions. They are indebted to Professor Y. Fukushima for his help in numerical computations. Computations were done at the Computing Center of Kyushu University with the computer FACOM-M382 with the financial support of Institute for Nuclear Study, University of Tokyo.

APPENDIX

In this appendix we discuss the movement of the zero of anomalous absorption on the complex-k plane when the Coulomb potential is reduced to 0 after the imaginary potential is turned off.

Let us first discuss the case of $l=0$. The movement of the zero is shown in Fig. 3, from point P to point B on curve (a). In order to elucidate the movement, it is useful to consider the movement of the pole associated with the zero. The pole is at the complex conjugate of the zero since the potential is real after point P. It is a resonance pole until the zero reaches the imaginary axis, and becomes a bound state pole thereafter.

A remarkable feature of the movement of the zero is that it approaches the origin, $k=0$, tangentially to the real-k axis. This may be understood as follows. First, one notes that the zero cannot be in the fourth quadrant in any case, for otherwise the conjugate pole would be in the first quadrant, which is impossible. Hence, the zero cannot reach the negative imaginary axis directly through the fourth quadrant.

Second, it cannot directly reach the positive imaginary axis either. In fact, if the zero is in the first quadrant at k, the conjugate pole at k^* is a resonance pole and its energy $E=\hbar^2k^{*2}/2\mu$ is complex: $E\equiv E_0-i\Gamma/2$ with $\Gamma>0$. The observed energy and the width of the resonance are given by E_0 and Γ, respectively. Figure 3 shows that as N_C decreases $|k|$, and hence the corresponding observed energy E_0, decreases. It turns out that the rate of decrease of E_0 is greater than that of N_C. As a consequence, E_0 eventually becomes lower than the Coulomb barrier height B_C at the potential surface. Then, the width of the resonance, Γ, becomes extremely small, as is well known, and tends to 0 in the limit of

$E_0 \to 0$. Thus, the resonance reaches the origin tangentially to the real axis, and so does the associated zero.

It should be noted that $k=0$ is actually an essential singularity of $S_{lj}^N(k)$; $\lim_{k\to 0} S_{lj}^N(k)$ depends on the way k approaches 0. For example, if k approaches 0 on the real axis, instead of tangentially, the limit is 1 instead of 0 because of the unitarity of the S matrix for real k.

The essential singularity of $k=0$ calls for special caution in determining the movement of the zero after it reaches the imaginary axis, whether it moves upward or downward. The fact that it actually moves downward can be confirmed by giving the potential a small imaginary part, instead of making it exactly real.[5] Another way of confirming this is to turn off the Coulomb potential first and then the imaginary potential. The locus of the zero in that case is found to be *AQB* on curve (a) in Fig. 3. There is no essential singularity on this locus.

Once the zero starts moving downward from the origin, it keeps doing so until point B at $N_C=0$. The reason for this is easily understood if one again considers the movement of the conjugate pole. Since the Coulomb potential is repulsive, the net potential becomes more attractive as the strength of the Coulomb potential decreases. As a consequence, the binding energy of the bound state corresponding to the pole increases. Hence, the pole moves upward. The zero which is its complex conjugate must, therefore, move downward.

For $l\neq 0$ the movement of the zero, shown in Fig. 3 by curve (a'), is qualitatively the same as for $l=0$, but the zero does not reach the imaginary axis and stops at a point, B', in the first quadrant at $N_I=N_C=0$. Hence, the zero is of type R just as in the case of the neutron.

[1]M. Kawai and Y. Iseri, Phys. Rev. C 31, 400 (1985).
[2]F. D. Becchetti and G. W. Greenlees, Phys. Rev. 182, 1190 (1969).
[3]W. Cassing, M. Stingl, and A. Weiguny, Phys. Rev. C 26, 22 (1982).
[4]See, e.g., G. R. Satchler, *Direct Nuclear Reactions* (Oxford University Press, Oxford, 1983), Chap. 12, p. 500.
[5]K. W. McVoy, in *Fundamentals in Nuclear Theory* (IAEA, Vienna, 1967), Chap. 8, p. 419.